iScience

CellPress
OPEN ACCESS

Article

Mycobacterial CpsA activates type I IFN signaling in macrophages via cGAS-mediated pathway

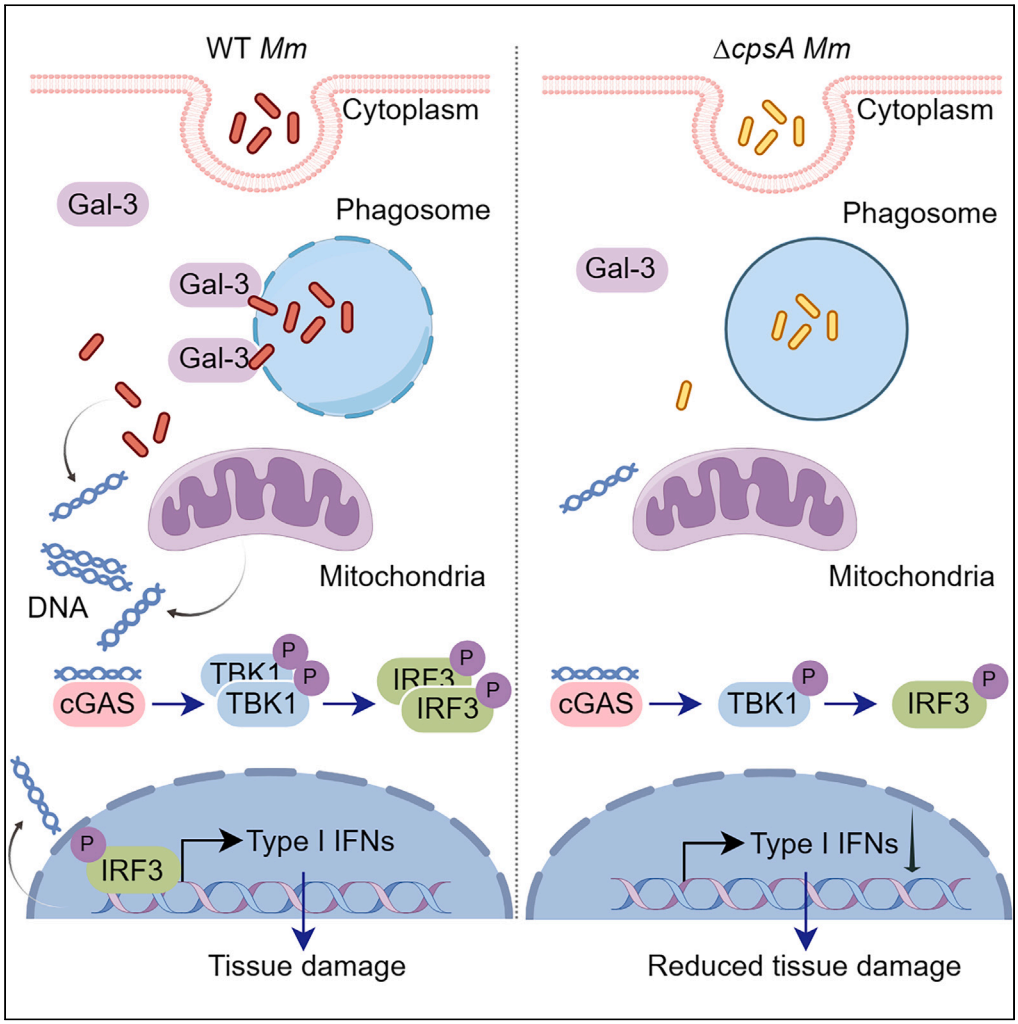

Yue Ding, Jingfeng Tong, Geyang Luo, ..., Qi Chen, Bo Yan, Qian Gao

haipengliu@tongji.edu.cn (H.L.)
chenqi@fjnu.edu.cn (Q.C.)
bo.yan@shphc.org.cn (B.Y.)
qiangao@fudan.edu.cn (Q.G.)

Highlights

CpsA boosts mycobacterial infection-induced type I IFN production and pathology

CpsA induces type I IFN production by activating cGAS-TBK1-IRF3 signaling axis

CpsA triggers phagosomal membrane rupture and the release of host and bacterial DNA

Ding et al., iScience 27, 109807
May 17, 2024
https://doi.org/10.1016/j.isci.2024.109807

iScience

CellPress
OPEN ACCESS

Article

Mycobacterial CpsA activates type I IFN signaling in macrophages via cGAS-mediated pathway

Yue Ding,[1,8] Jingfeng Tong,[1,8] Geyang Luo,[1] Rongfeng Sun,[1] Cheng Bei,[1] Zhihua Feng,[2] Lu Meng,[3] Fei Wang,[4] Jing Zhou,[5,6] Zihan Chen,[5,6] Duoduo Li,[5] Yufeng Fan,[1] Shu Song,[5] Decheng Wang,[6] Carl G. Feng,[7] Haipeng Liu,[4,*] Qi Chen,[2,*] Bo Yan,[5,*] and Qian Gao[1,9,*]

SUMMARY

Type I interferon (IFN) production is crucial in tuberculosis pathogenesis, yet the bacterial factors initiating this process are incompletely understood. CpsA, protein of *Mycobacterium marinum and Mycobacterium tuberculosis*, plays a key role in maintaining bacterial virulence and inhibiting host cell LC3-associated phagocytosis. By utilizing CpsA full deletion mutant studies, we re-verified its essential role in infection-induced pathology and revealed its new role in type I IFN expression. CpsA deficiency hindered IFN production in infected macrophages *in vitro* as well as zebrafish and mice *in vivo*. This effect was linked to the cGAS-TBK1-IRF3 pathway, as evidenced by decreased TBK1 and IRF3 phosphorylation in CpsA-deficient bacterial strain-infected macrophages. Moreover, we further show that CpsA deficiency cause decreased cytosolic DNA levels, correlating with impaired phagosomal membrane rupture. Our findings reveal a new function of mycobacterial CpsA in type I IFN production and offer insight into the molecular mechanisms underlying mycobacterial infection pathology.

INTRODUCTION

Type I interferons (IFNs), comprising single IFNβ and multiple IFNα subtypes, have been well documented to play a critical role in host defense against viral infections. However, the role of type I IFNs during bacterial infections is more complicated, and it is generally accepted that type I IFNs can promote disease progression during *Mycobacterium tuberculosis* (*Mtb*) infection.[1–3] Active tuberculosis patients have a prominent induction of type I IFN blood transcript signatures, which correlate with disease severity.[4,5] Recently, a genetic mutation in IFN alpha/beta receptor subunit 1 was reported to be associated with decreased susceptibility to *Mtb* infection in humans.[6] Similarly, murine type I IFNs promote the mycobacterial intracellular growth,[7–9] and type I IFN receptor-deficient mice are more resistant to the infection by *Mtb* and virulent *M. bovis*.[10–14]

The host mechanisms responsible for type I IFN production during *Mtb* infection have been extensively studied. Cyclic GMP-AMP synthase (cGAS) has been shown to sense cytosolic DNA and initiate the production of type I IFN during mycobacterial infection.[15–18] The engagement of cGAS by DNA activates stimulator of interferon genes (STING) followed by the activation of TANK-binding kinase 1 (TBK1), which in turn induces the activation of transcription factors, including NF-κB and IRF3, essential for the induction of type I IFNs.[19,20]

One of the mycobacterial type VII secretion systems, ESX-1, has been documented as a major bacterial factor required for type I IFN production.[17,21,22] ESX-1 system-mediated type I IFN induction is mainly associated with increasing nucleic acids in the cytoplasm, either DNA or RNA.[17,23] The observation showing the coprecipitation of bacterial-specific DNA fragments and cGAS has led to the suggestion that bacterial DNA released into the cytosol was the main trigger of type I IFN production in early studies.[17] However, more recent reports have provided an alternative perspective that host-derived mitochondrial or nuclear DNA was the main source of cytosolic DNA during *Mycobacterium*

[1]Key Laboratory of Medical Molecular Virology (MOE/NHC/CAMS), School of Basic Medical Sciences, Shanghai Medical College, Shanghai Public Health Clinical Center, Fudan University, Shanghai, China
[2]Fujian Key Laboratory of Innate Immune Biology, Biomedical Research Center of South China, Fujian Normal University Qishan Campus, Fuzhou, China
[3]The Center for Microbes, Development and Health, Key Laboratory of Molecular Virology & Immunology, Institute Pasteur of Shanghai, Chinese Academy of Sciences/University of Chinese Academy of Sciences, Shanghai, China
[4]Shanghai Key Laboratory of Tuberculosis, Shanghai Pulmonary Hospital, Tongji University School of Medicine, Shanghai, China
[5]Shanghai Public Health Clinical Center, Fudan University, Shanghai, China
[6]Hubei Key Laboratory of Tumor Microenvironment and Immunotherapy, College of Basic Medical Sciences; Institute of Infection and Inflammation, College of Basic Medical Sciences, China Three Gorges University, Yichang 443002, P.R China
[7]Immunology and Host Defence Laboratory, School of Medical Sciences, Faculty of Medicine and Health, The University of Sydney, Camperdown, NSW, Australia
[8]These authors contributed equally
[9]Lead contact
*Correspondence: haipengliu@tongji.edu.cn (H.L.), chenqi@fjnu.edu.cn (Q.C.), bo.yan@shphc.org.cn (B.Y.), qiangao@fudan.edu.cn (Q.G.)
https://doi.org/10.1016/j.isci.2024.109807

marinum (*Mm*) or *Mtb* infection.[18,24,25] Regardless, the damage of phagosomes remains as a prerequisite for the release of DNA.[18] It remains unclear whether additional bacterial components are also capable of triggering type I IFN production.

CpsA has been demonstrated to be an important virulence-related protein in both *Mtb* and *Mm* by others and us.[26–29] In addition, a recent study has shown that CpsA functions as a secreted protein that suppresses LC3-associated phagocytosis (LAP) by inhibiting the recruitment of NADPH oxidase in macrophages.[29] However, whether CpsA manipulates other host signaling pathways is unknown.

By employing a CpsA full deletion mutant Δ*cpsA Mm* and two distinct animal models, we demonstrate that CpsA deficiency leads to less inflammatory cell infiltration and tissue damage *in vivo*. RNA sequencing (RNA-seq) analysis revealed a significantly reduced type I IFN signaling in macrophages infected with Δ*cpsA Mm*. Importantly, we established an essential role for cGAS-TBK1-IRF3 axis and host and *Mm* DNA in CpsA-induced type I IFN production in macrophages. Our findings reveal a previously unknown function of mycobacterial CpsA in type I IFN production and tissue inflammation, providing a potential drug target for anti-tuberculosis (TB) drug development.

RESULTS

CpsA is indispensable for mycobacterial infection-induced pathology

Previously, we reported that a transposon insertion CpsA mutant leads to decreased virulence.[26] To further eliminate the potential interference caused by the CpsA-truncated protein and perform a more detailed pathological analysis, we generated a new CpsA full deletion mutant Δ*cpsA Mm* with complete depletion of *cpsA* open reading frame (Figures S1A–S1E). Δ*cpsA Mm* causes an intracellular growth defect resembling that of our previous studies (Figure S2). Following intraperitoneal infection of adult zebrafish with wild-type (WT) and Δ*cpsA Mm* strains, we observed that the animals injected with WT *Mm* displayed more extensive abdominal swelling and gross granuloma formation in livers than their Δ*cpsA Mm*-injected counterparts as previously reported (Figures S3A and S3B). Moreover, careful pathological examination revealed that the massive tissue immunopathology, characterized by the accumulation of necrotic cells and infiltrating leukocytes, was present only in the livers of WT *Mm*-infected zebrafish (Figure 1A). The severe tissue inflammation associated with WT *Mm* was confirmed by a mouse tail vein *Mm* infection model. While all infected tails showed some degree of ulceration, mice infected with WT *Mm* exhibited more extensive tissue damage. The ulcerations caused by the WT strain are long and continuous, in contrast to the punctate and separated ulcerations observed in mice infected with the knockout strain (Figure 1B). This observation is consistent with the statistical analysis of the ulceration areas, which showed that the WT *Mm*-infected group was significantly larger than the Δ*cpsA Mm* group (Figure 1C). H&E staining and inflammatory cell counts revealed a much more extensive inflammatory cell infiltration in WT *Mm*-infected mouse tails compared to the mutant group (Figures 1D and 1E). Together, these data showed that CpsA contributes to *Mm*-induced immunopathology.

CpsA activates type I IFNs signaling in *Mm*-infected macrophages

To further identify the research direction for enhanced tissue inflammation in CpsA-competent *Mm*-infected host, we performed RNA-seq analysis on WT and Δ*cpsA Mm*-infected mouse macrophages. To minimize the impact of different bacterial loads on gene expression patterns, we collected RNA samples at 4 h post infection (hpi) when intracellular bacterial loads were comparable between the two groups (Figure 2A). The WT and Δ*cpsA Mm* samples were well distinguished through multidimensional scaling (Figure 2B). We observed that only a few genes were induced differentially between these two groups, with 10 upregulated and 11 downregulated genes in macrophages infected with Δ*cpsA Mm* compared to those infected with WT *Mm* (Figures 2C and 2D). Among the 10 upregulated genes, *Flt3l*, *Nhej1*, and *Fer1l5* have been suggested to be required for macrophage survival, DNA damage repair, and cell membrane repair, respectively,[30–33] suggesting WT *Mm*-infected macrophages undergo more extensive cell death commonly coupled with DNA and cell membrane damage. Unexpectedly, the expression of *Ifnb1* and two interferon-stimulated genes (ISGs), namely *Ifit1* and *Ifit3b*, were induced at a significantly lower level in Δ*cpsA Mm*-infected cells than their WT *Mm*-infected counterparts (Figures 2C and 2D).

Given that type I IFNs are closely associated with immunopathology and cell deaths,[9,13] we suspected that preferential induction of type I IFNs might, at least partially, explain the different pathological phenotypes observed. Quantitative reverse-transcription PCR (RT-qPCR) was performed to further confirm our RNA-seq findings. Δ*cpsA Mm* failed to induce sustained *Ifnα* and *Ifnβ* mRNA expression at early time points (6 and 10 hpi), whereas infection of macrophages with WT *Mm* and the *cpsA* complemented strain resulted in a robust induction of *Ifnα* and *Ifnβ* mRNA, with a peak production of mRNA at 10 hpi (Figures 3A and 3B). Similar to *Ifnα* and *Ifnβ* mRNA, the induction of *Cxcl10* and other ISG mRNA was also impaired (Figures 3C and 3D). Consistently, the protein level of IFNβ in the supernatants of Δ*cpsA Mm*-infected macrophage cultures was also significantly lower than those of WT *Mm* and Δ*cpsA*::*cpsA Mm*-infected macrophage cultures (Figure 3E). Considering the transcription regulation of *Il-1β* is preferentially suppressed by type I IFNs,[34] we also analyzed the expression kinetics of *Il-1β* induction. Indeed, the mRNA levels and the protein level of *Il-1β* in *ΔcpsA Mm*-infected macrophages were significantly higher than those of WT and the complemented strains (Figures 3F and 3G). Finally, we examined the survival of macrophages infected with WT *Mm*, Δ*cpsA Mm*, and Δ*cpsA*::*cpsA Mm* at 1 and 2 days post-infection. As expected, the extent of cell lysis in Δ*cpsA Mm*-infected macrophage cultures was much lower than those of WT *Mm* and Δ*cpsA*::*cpsA Mm*-infected cells (Figure 3H). Together, these data indicated that CpsA is required for the induction of type I IFNs and contributes to the pathological tissue damage caused by *Mm in vivo*.

CpsA contributes to *in vivo* expression of type I IFN and ISGs

Considering the close relationship between type I IFN and *Mtb*-induced pathology, we next sought to determine the role of CpsA in type I IFN induction following infection *in vivo*. Consistent with the milder pathological manifestation described earlier, type I IFNs and ISG induction

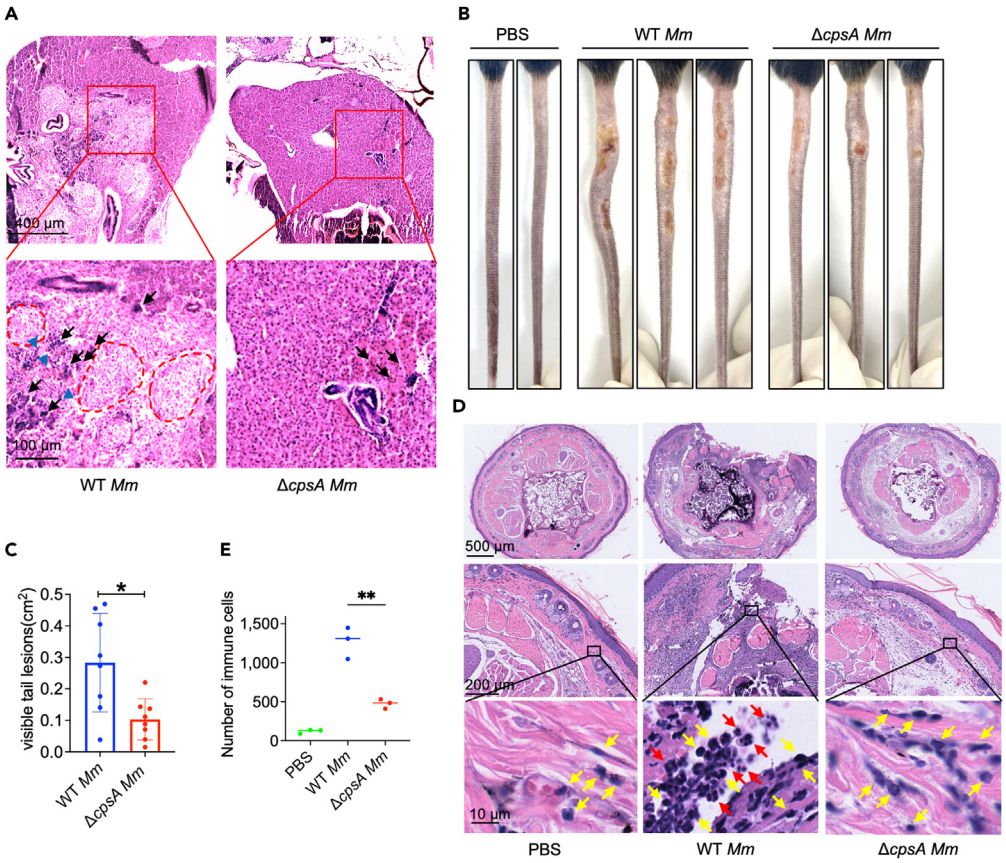

Figure 1. CpsA is required for histopathological injury both in zebrafish and mouse tail infection models

(A) Histopathology of the infected zebrafish at 8 dpi with WT *Mm* or Δ*cpsA Mm*. Infected fish were subjected to histological analysis with hematoxylin and eosin (H&E) staining. Black arrows indicate infiltrated inflammation cells. Blue arrowheads indicate necrosis cells. Red circle region indicates the granuloma. The analysis was conducted using two fish per group, with two samples per fish, and three sections examined per sample.

(B) C57BL/6J mice were infected with WT *Mm* or Δ*cpsA Mm* via tail vein injection, PBS as control. Whole tails were photographed at 10 dpi.

(C) The total area of visible tail lesions were calculated by measuring the length and width of lesions. Data were shown as mean size ± SEM ($n = 8$), *$p < 0.05$ by Mann-Whitney rank-sum test.

(D) Representative histopathology images of tails from WT *Mm* or Δ*cpsA Mm*-infected C57BL/6J mice at 10 dpi. Uninfected and infected tails were subjected to histological analysis with H&E staining. Yellow arrows indicate infiltrated macrophages and red arrows indicate infiltrated neutrophils.

(E) The infiltrated immune cells in histopathology images of mice tails were counted. The analysis was performed using three mice per group, with two samples from different tissues per mouse, and three sections examined per sample. Data were shown as mean size ± SEM, **$p < 0.01$ by one-way ANOVA.

was greatly diminished in Δ*cpsA Mm*-infected adult zebrafish (Figure 4A). Notably, the expression of most members of type I IFNs (*ifnphi1*, *ifnphi2*, *ifnphi3*) and ISGs (*irgf1*, *irgf3*, *irgq1*, *irge4*) increased gradually along with the progression of the infection except *irge2*, suggesting that pathogen loads *in vivo* are also an important factor for inducing type I IFN signaling (Figure 4A). To confirm the CpsA plays a similar regulatory role in type I IFN production in mammalian host, we performed mouse tail vein infection with WT or Δ*cpsA Mm* strains. The reduced productions of *Ifnβ* and several ISGs (*Ifi1*, *Ifit1*, *Ifi213*) were also observed in Δ*cpsA Mm*-infected mouse tissues 10 days after infection (Figure 4B). Together, these results suggest that mycobacterial CpsA is responsible for the type I IFN signaling activation and associated pathological tissue damage *in vivo*.

CpsA induces type I IFN production by activating cGAS-TBK1-IRF3 signaling axis

Considering the cytosolic DNA sensor cGAS has been shown to play an important role in triggering type I IFN expression in macrophages during mycobacterial infection,[17] we interrogated whether cGAS is responsible for CpsA-mediated type I IFN production. Since we did not have access to the $Cgas^{-/-}$ RAW264.7 cell line, we opted to utilize $Cgas^{-/-}$ mouse bone-marrow-derived macrophages (BMDMs) instead. $Cgas^{+/+}$ WT and $Cgas^{-/-}$ mouse BMDMs were infected with WT or Δ*cpsA Mm* and *Ifnβ* expression was measured by RT-qPCR at 10 hpi. In consistence with the infection experiments using RAW264.7 cell line (Figure 3A), in $Cgas^{+/+}$ WT BMDMs Δ*cpsA Mm* induced significantly lower level of *Ifnβ* compared to CpsA-competent *Mm*. However, this difference was diminished in $Cgas^{-/-}$ BMDMs (Figure 5A), suggesting that CpsA protein-mediated type I IFN production is cGAS dependent.

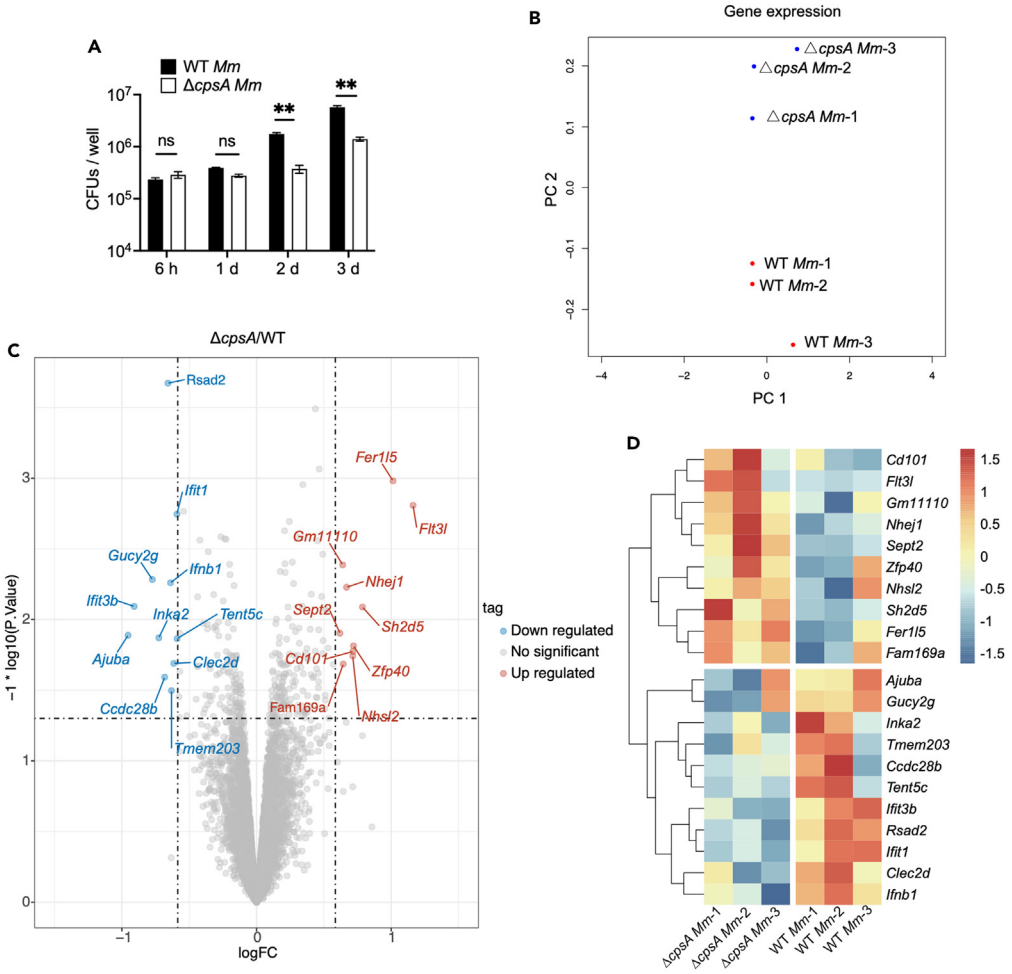

Figure 2. Results of RNA-seq analysis and differentially expressed genes

(A) Colony-forming unit (CFU) counts of intracellular bacteria in RAW264.7 macrophages infected with WT *Mm* and Δ*cpsA Mm* with MOI of 10. Data are representative of three independent experiments and values are presented as means ± SEM. $^{**}p < 0.01$ by two-way ANOVA with multiple comparisons.

(B) Multidimensional scaling between WT *Mm* and Δ*cpsA Mm*-infected RAW264.7 macrophages. Each group has three biological replicates.

(C) Volcano plot of macrophage differentially expressed genes (DEGs). Colored plots stand for genes with significant differences ($p < 0.05$). Red plots stand for upregulated genes of RAW264.7 infected with Δ*cpsA Mm* compared to WT *Mm* while blue plots stand for downregulated genes. The x axis represented log2 of fold change and the y axis represented the log10 of *p* values.

(D) Heatmap showing the expression profile of selected DEGs with $> |2 - fold|$ higher expression in WT *Mm* than Δ*cpsA Mm* infection. The gene expression levels were normalized using the *Z* score method. The color of each block represents the *Z* score value of gene expression, which indicates the degree of deviation of each gene across all samples relative to the average expression of that gene across all samples.

TBK1 is the key component required for type I IFN production, as it mediates all major signaling pathways responsible for the cytokine production. TBK1 phosphorylation leads to the phosphorylation of other downstream transcriptional factors, such as IRF3.[35] As expected, we found that the level of phosphorylated TBK1 in Δ*cpsA Mm*-infected macrophages was markedly lower than that in WT *Mm*-infected macrophages at 3, 4, and 6 hpi (Figures 5B and 5C). During mycobacterial infection, the transcription factors activated by TBK1 include IRF3 and NF-κB, the activation of which will result in their nuclear translocation.[20] Interestingly, we observed that while the protein level of IRF3 in nuclear fractions was significantly lower in Δ*cpsA Mm*-infected macrophages at 2 and 4 hpi (Figures 5D and 5E), no significant differences in NF-κB (p65) expression were found (Figure 5F). To further rule out the role of NF-κB pathway in TBK1-dependent innate response, the kinetics of several NF-κB-regulated cytokines were also examined and no difference was observed (Figures S4A–S4C). Together, these data suggest that CpsA-mediated type I IFN production is via cGAS-TBK1-IRF3 pathway.

CpsA triggers the phagosomal membrane damage

The main source of the cytosolic DNA eliciting type I IFN production during virulent mycobacterial infection in macrophages remains controversial.[18,23–25] Thus, we examined the releases of both host and bacterial DNA into the cytoplasm of WT and Δ*cpsA Mm*-infected

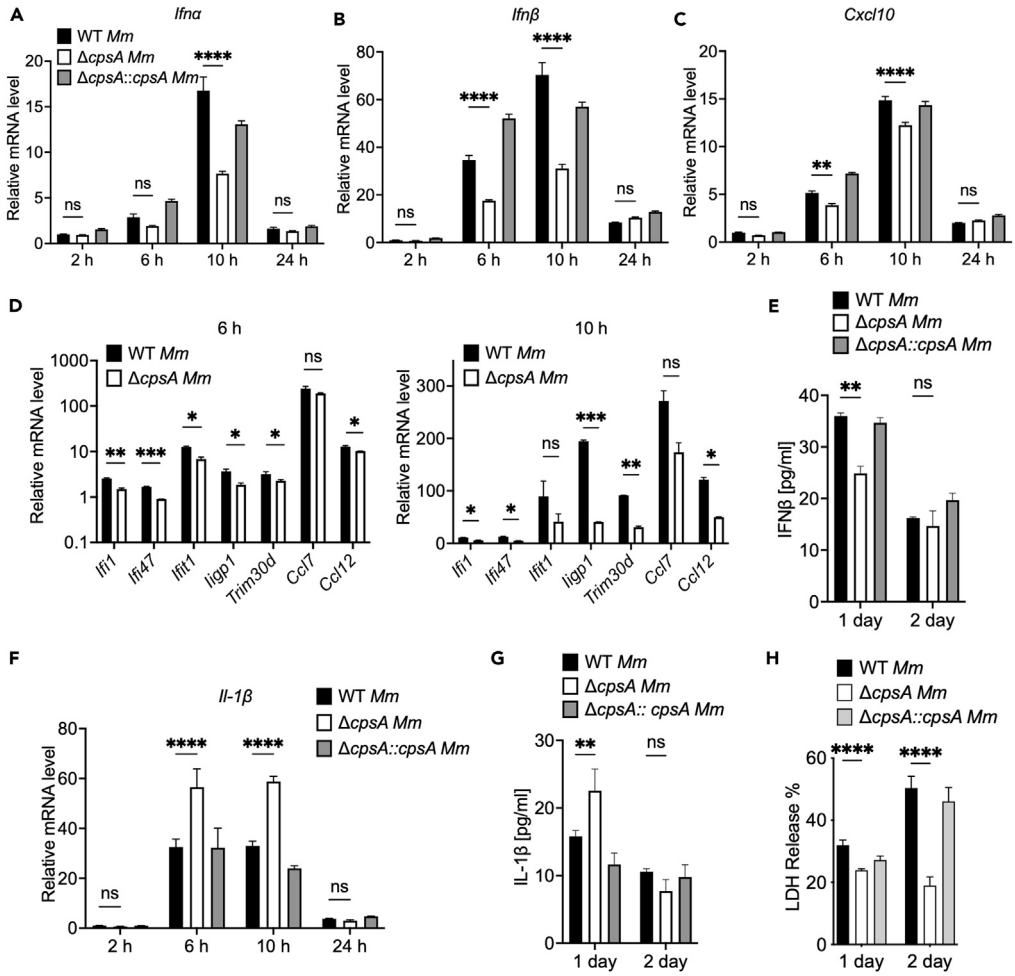

Figure 3. Induction of type I IFNs and ISGs in RAW264.7 cells are dependent on CpsA

RAW264.7 cells were infected with WT, Δ*cpsA*, and the complemented strains at MOI of 10. RNA was isolated at 2, 6, 10, and 24 hpi. (A) *Ifnα* (the primers detected the combined expression of *Ifnα* subtype 1 and *Ifnα* subtype 7), (B) *Ifnβ*, (C) *Cxcl10*, and (F) *Il-1β* levels were determined by RT-qPCR, and values were normalized to *Gapdh* and WT strain at 2 hpi.

(D) RAW264.7 cells were infected with WT, Δ*cpsA Mm* strains at MOI of 10. RNA was isolated at 6 and 10 hpi. The mRNA levels of *Ifi1*, *Ifi47*, *Ifit1*, *Iigp1*, *Trim30d*, *Ccl7*, and *Ccl12* were determined by RT-qPCR, and values were normalized to *Gapdh* and uninfected RAW264.7 cells.

(E) Supernatants were collected from infections at 1 dpi and 2 dpi and were subjected to ELISA for analysis of IFNβ protein concentration.

(G) Supernatants were collected from infections at 1 dpi and 2 dpi and were subjected to ELISA for analysis of IL-1β protein concentration.

(H) RAW264.7 cells infected with WT, Δ*cpsA*, and the complemented strains at MOI of 10 were analyzed by LDH release assay. Shown is a representative experiment of three (n = 3). Data represent means ± SEM of three independent experiments. *p < 0.05; **p < 0.01; ***p < 0.001; ****p < 0.0001; ns, not significant. Two-way ANOVA with multiple comparisons test for A, B, C, E, F, G, and H, unpaired t tests for D.

macrophages and found that infection with WT *Mm* induced a significantly higher amount of both host mitochondrial, nuclear, and bacterial DNA (Figure 6A). Mitochondrial protein TIMM44 and nuclear protein Histone H3 were assessed to exclude the possible artificial effects due to autolysis during fractionation procedure (Figure 6B).

The type I IFN production is closely associated with phagocytosis of mycobacteria and phagosomal membrane rupture, but the underlying mechanism remains unclear.[18,36] Therefore, we speculate that CpsA might also involve in the phagosomal membrane permeabilization. Galectin-3 was employed as a marker to indicate phagosome membrane rupture, with its cytoplasmic dispersion under normal conditions transitioning to rapid accumulation near the ruptured phagosome following the breakdown of a phagosome containing bacteria.[37–39] The immunofluorescence visualization of galectin-3 expression patterns demonstrated cytoplasmic localization consistent with prior research. Furthermore, the observation of colocalized galectin-3 point-like aggregation around ruptured phagosomes containing bacteria was noted (Figure 6C). Analysis of the colocalization of bacteria and galectin-3 indicated a significantly lower recruitment of galectin-3 to *Mm* containing phagosomes in Δ*cpsA Mm*-infected macrophages than their WT *Mm*-infected counterparts (Figures 6C and 6D). These results suggested CpsA is indispensable for mycobacteria infection-induced phagosome membrane damage and is a bacterial factor linking phagosomal integrity and type I IFN production.

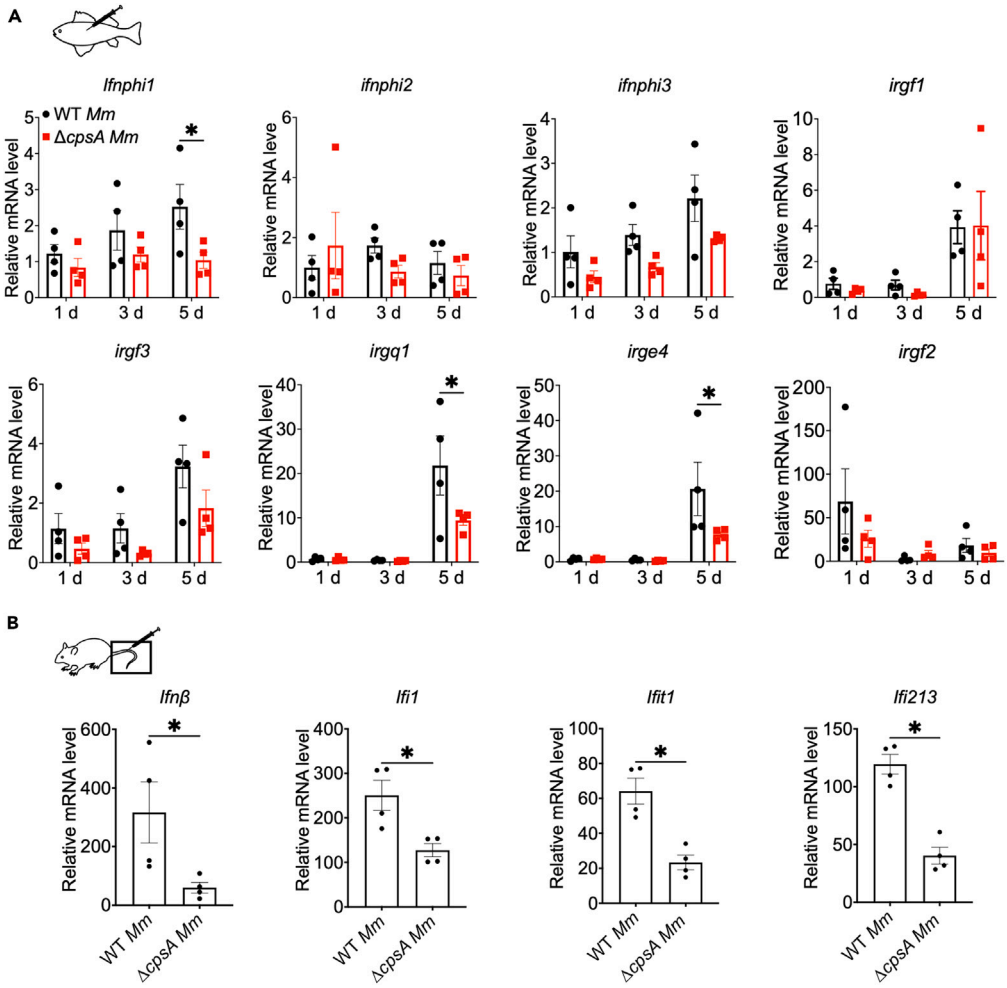

Figure 4. CpsA-dependent type I IFNs and ISGs activation *in vivo*

(A) Adult zebrafishes were infected with WT or Δ*cpsA Mm* strains (10^4 CFU) and the mRNA levels of type I IFNs and ISGs of the fish body were determined by RT-qPCR and normalized to *gapdh*.

(B) C57BL/6J mice were infected with WT, Δ*cpsA Mm* strain (~3 × 10^8 CFU/mouse) via tail vein injection. The mRNA levels of type I IFNs and ISGs of the tail were determined by RT-qPCR. In A and B, data shown are mean fold increase over PBS-treated animals ± SEM. A, *$p < 0.05$ by two-way ANOVA with multiple comparisons test, and B, *$p < 0.05$ by unpaired t tests.

DISCUSSION

Type I IFNs are known to contribute to mycobacterial disease pathogenesis in diverse range of hosts.[1] Although ESX-1 secretion system has been reported to be indispensable for the cytokine production,[18,40] specific mycobacterial molecules responsible for triggering type I IFN expression and the underlying mechanisms have yet to be determined. CpsA has been previously identified as a mycobacterial virulence-related factor required for pathogen proliferation *in vivo* and inhibiting LAP induction in host macrophages.[26,28,29] In this study, by taking advantage of different *in vitro* and *in vivo* infection models and RNA-seq approach, we uncovered a novel role for CpsA in type I IFN production and infection pathogenesis. We also demonstrate that CpsA is involved with the rupture of the macrophage phagosome that is associated with cGAS-TBK1-IRF3 signal axis-dependent type I IFN production.

In our previous study, we have found that the transposon insertion CpsA mutant *Mm* strain infection causes significantly lower bacterial load and fewer granulomas in the adult zebrafish infection model.[26] To further eliminate the potential interference caused by the truncated protein, we infected zebrafish with a newly generated *cpsA*-null mutant Δ*cpsA Mm* and found a similar phenotype. In addition, less inflammatory cell infiltrations and tissue damages were observed in animals infected with Δ*cpsA* mutant using both zebrafish infection model and mouse tail vein infection model, in which Mm primarily infects the tail skin where the temperature is suitable for the bacterial growth.[41]

Unexpectedly, we found that CpsA plays a previously unrecognized role in type I IFN production. In both zebrafish and mouse models, we observed a decrease in the expression levels of type I IFN genes and ISGs in Δ*cpsA Mm*-infected group. We found that the ISGs associated with CpsA in zebrafish are different from those in mice, which we speculate may be due to evolutionary variations between fish and

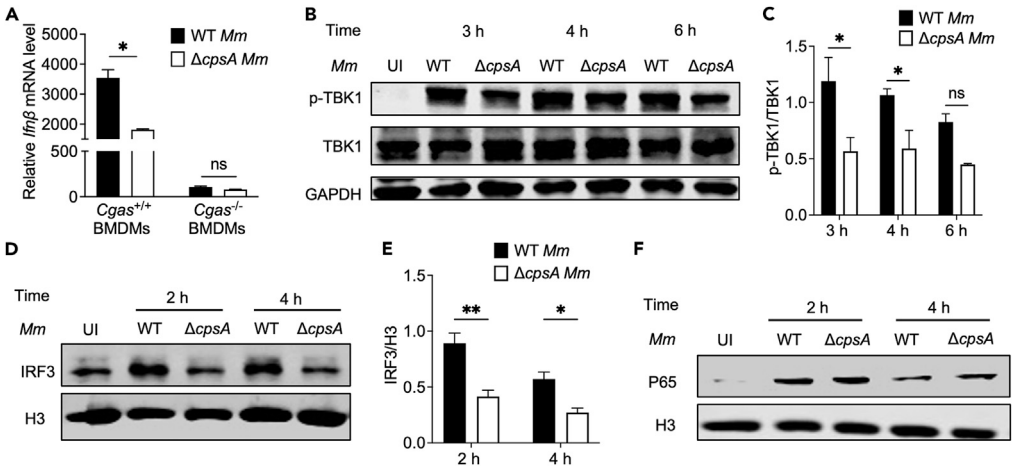

Figure 5. CpsA-related type I IFN production is through cGAS-TBK1-IRF3 pathway

(A) BMDMs extracted from WT mice or *Cgas* knockout mice were infected with WT or Δ*cpsA Mm* strains at MOI of 10. RNA was isolated at 10 h after infection. *Ifnβ* levels were determined by RT-qPCR in different infection cells; values were normalized to *Gapdh* and uninfected BMDMs.

(B) RAW264.7 cells were infected with WT and Δ*cpsA* strains at MOI of 10. Total cell lysates and nuclear part were harvested at indicated time points. Phospho-TBK1 and TBK1 protein levels were determined by using a densitometer and (C) corresponding statistical results were calculated from two independent experiments by ImageJ software, GAPDH as a reference protein.

(D) The protein levels of IRF3 from nuclear fraction were determined by western blot (WB) and (E) corresponding statistical results were calculated from two independent experiments by ImageJ software, H3 as a reference.

(F) Nuclear p65 and H3 protein levels were determined by WB. Shown is a representative experiment of three. Data represent means ± SD of three independent experiments. A, $*p < 0.05$, ns, not significant by unpaired t test, and C, D $*p < 0.05$, $**p < 0.01$, ns, not significant by two-way ANOVA with multiple comparisons test.

mammalian given the existence of a unique type of virus-induced IFNs in fish.[42] Although the differences of type I IFN signaling *in vivo* might also attribute to an indirect effect of CpsA on bacterial proliferation, the significant decreased type I IFN expressions in Δ*cpsA Mm*-infected macrophages at early time points when bacteria barely proliferated demonstrated a potent role of CpsA in inducing type I IFNs. Given that type I IFN production is closely associated with mycobacterial-induced pathology,[5,9,13] our findings suggest that CpsA may regulate the pathogenesis of mycobacterial diseases. Further analysis of its expression in clinical isolates could facilitate the understanding of infection transmission and the clinical outcome of the disease.

Defining the underlying mechanisms for mycobacterium-induced type I IFNs is critical for the understanding of TB disease progression and pathology. cGAS-STING-TBK1-IRF3 signaling pathway remains to be the central player. For example, Watson et al. demonstrated TRIM14 is a key negative regulator of *Ifnβ* and ISGs expression via interacting with cGAS and TBK1 directly during *Mtb* infection.[43] Sun et al. found an *Mtb* determinant, MmsA, can hinder the type I IFN response via interacting with STING.[8] Here, our data also showed that cGAS plays a critical role in CpsA-induced type I IFN production, as the difference in macrophage type I IFN production diminished in the absence of cGAS. Whether CpsA directly or indirectly interacts with cGAS during this process warrants further investigation in the future. Here, we also noted that the transcription regulator, IRF3 but not NF-κB was affected in a CpsA-dependent way. The phenomenon of double-stranded DNA (dsDNA)-induced IRF3 activation, without affecting NF-κB, also appeared on PPP6C, which is a negative regulator for dsDNA-induced IRF3 activation in viral infection.[44] Ni et al. have also reported that ubiquitination of STING on K224 is essential for activation of IRF3 but not NF-κB,[45] which suggests CpsA might affect the modification of proteins in cGAS-STING-TBK1-IRF3 pathway.

cGAS is the nucleic acid-sensing receptor in the cytoplasm, recognizing DNA released into the cytosol from host or invaded microorganisms. To date, the main source of the cytosolic DNA contributing to the cGAS-mediated downstream signaling in macrophages infected with *Mtb* remains controversial. By using cGAS precipitation combined with nucleic acid detection method, early research demonstrated that bacterial DNA was the main ligand of cGAS.[17] However, recent studies provide alternative views that host-derived DNA, rather than mycobacterial DNA, plays a key role in type I IFN production.[18,24] Interestingly, our experiment illustrates that both host-derived and bacterial DNA play a role in the heightened production of type I IFNs in WT *Mm*-infected macrophages, as opposed to those infected with Δ*cpsA Mm*. The contribution of different sources of cytosolic DNA in activating cGAS pathway in our setup warrants investigation in the future. Interestingly, previous studies have demonstrated that the augmented release of mitochondrial and nuclear DNA suggests a potential role in destabilizing mitochondria and promoting increased cellular mortality.[18,24] In consistent with previous findings, we also observed that CpsA-deficient strains lead to reduced cell death in macrophages, which might also partially contribute to the less severe tissue damage observed in animal models. Nevertheless, further investigations are required to elucidate the precise impact of CpsA on mitochondrial stability, cell death, and its potential contribution to pathogenicity.

Previously, Stefan et al. have demonstrated that *Mtb* CpsA hinders LAP by inhibiting the recruitment of NADPH oxidase, thus blocking the maturation of phagosome-lysosome fusion and leading to the proliferation of *Mtb* in macrophages successfully.[29] Here we showed that CpsA

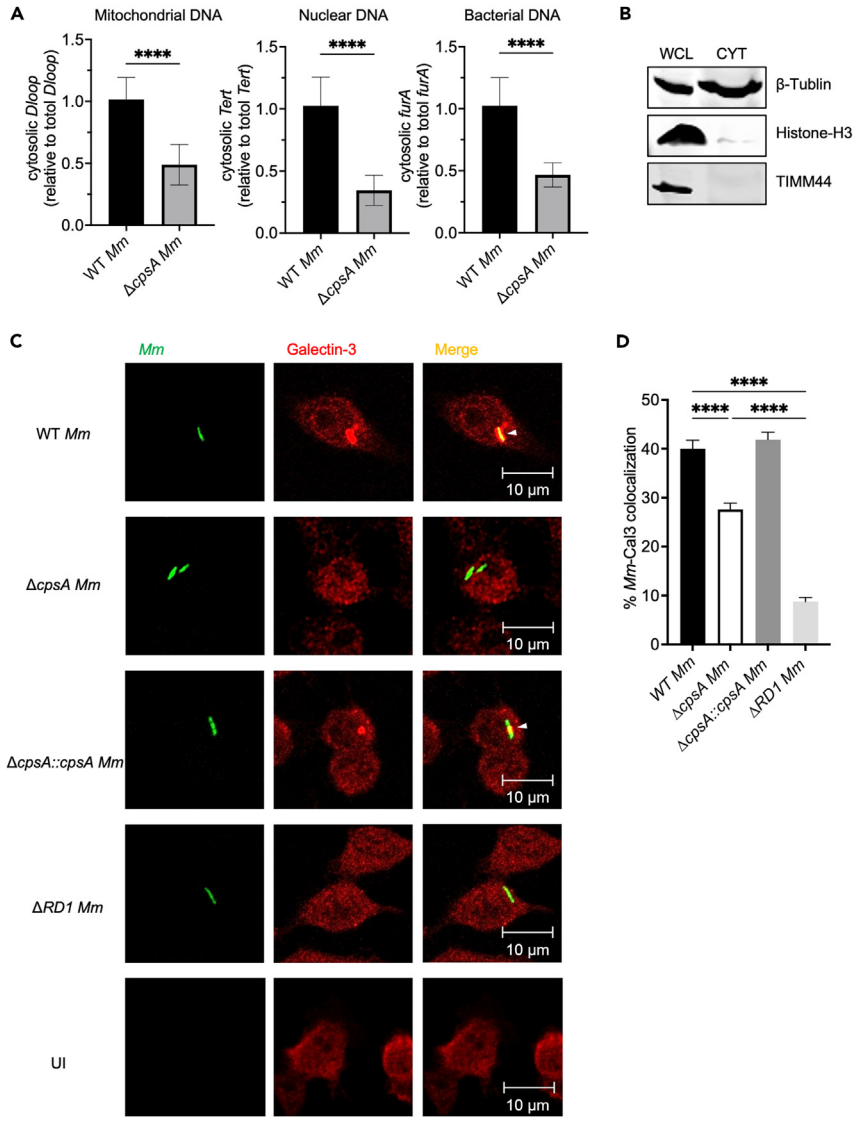

Figure 6. CpsA is required for the recruitment of galectin-3 to the *Mm* containing phagosomes followed by release of host and bacterial-derived DNA to the cytosol

(A) The levels of mitochondrial (*D loop1*), nuclear (*Tert*), or *Mm* (*furA*) DNA in the cytosolic compartment of RAW264.7 cells infected with WT or Δ*cpsA Mm* were analyzed by qPCR as described in materials and methods. Data represent means ± SD. ****$p < 0.0001$ by unpaired t test.

(B) The mitochondrial protein TIMM44 and nuclear protein Histone H3 were analyzed in whole-cell lysates (WCL) and cytosolic fractions (CYT) by WB. GAPDH was used as a loading control.

(C) Immunofluorescence of RAW264.7 cells infected with Wasabi labeled WT, Δ*cpsA*, the complemented strains, and ΔRD1 *Mm* at MOI of 10 for 4 hpi with uninfected group as control and imaged after staining with anti-galectin-3 (red). Scale bar, 10 μm. White arrows indicate the colocalization of galectin-3 with bacteria.

(D) Quantification of *Mm* and galectin-3 colocalization in (C). A minimum of 200 cells were quantified per group. The images were representative of three independent experiments. Data represent means ± SD of three independent experiments. ****$p < 0.0001$ by one-way ANOVA.

protein participates in the rupture of the macrophage phagosome membrane thereby activating the expression of type I IFN. These work together suggested that CpsA facilitates mycobacterial intracellular growth by distinct mechanisms. Even though the current conclusions have only been validated in macrophage cell lines and animal models, the contribution of CpsA to human TB pathogenicity warrants further investigation.

In summary, we demonstrated that CpsA promotes the phagosomal damage and the activation of type I IFN signaling mediated by cGAS-TBK1-IRF3 pathway. The induction of type I IFNs is associated with the extensive tissue damage *in vivo*. Our study suggests CpsA could be a potential drug target, and precise functions of CpsA during host-mycobacterium interaction warrant further investigation.

Limitations of the study

The rupture of the phagosome is an essential process for mycobacterium to interact with the host cytoplasm, playing a crucial role in the survival of mycobacterium within the host and the TB disease progression. Our study unveils CpsA, a mycobacterial virulence protein, as a key player in promoting phagosome rupture. However, the precise mechanism underlying CpsA's facilitation of this process remains elusive.

STAR★METHODS

Detailed methods are provided in the online version of this paper and include the following:

- KEY RESOURCES TABLE
- RESOURCE AVAILABILITY
  - Lead contact
  - Materials availability
  - Data and code availability
- EXPERIMENTAL MODEL AND STUDY PARTICIPANT DETAILS
  - Animals
  - Cell culture
  - Mycobacterium strains and culture
- METHOD DETAILS
  - The *cpsA* knock out generation and complementation
  - Zebrafish infection
  - Mouse tail infection
  - Histology
  - RNA extraction and reverse-transcription quantitative PCR (RT-qPCR)
  - Infection of macrophages
  - RNA sequencing and transcriptome analysis
  - Western Blot
  - Immunofluorescence microscopy (IF)
  - Lactate dehydrogenase (LDH) release assay
  - Extraction of cytosolic DNA followed by qPCR
- QUANTIFICATION AND STATISTICAL ANALYSIS

SUPPLEMENTAL INFORMATION

Supplemental information can be found online at https://doi.org/10.1016/j.isci.2024.109807.

ACKNOWLEDGMENTS

This study was supported by grants from the National Natural Science Foundation of China (82272376 to Q.G.; 82372263 to B.Y.), the Shanghai Municipal Science and Technology Major Project (ZD2021CY001 to Q.G.), the Shanghai "Science and Technology Innovation Action Plan" Medical Innovation Research Special Project (22Y11920500 to B.Y.), and the China Postdoctoral Science Foundation (2020M681174 to J.T.). We thank Dr. L. Ramakrishnan for sharing *M. marinum* M strains.

AUTHOR CONTRIBUTIONS

Q.G. and B.Y. provided funding acquisition and were responsible for project administration; Y.D. and J.T. performed the experiments, analyzed the data, and prepared the article; G.L., R.S., C.B., Z.F., L.M., F.W., J.Z., Z.C., D.L. Y.F., and S.S. performed the experiments; C.G.F., H.L., Q.C., and D.W. designed the experiments; and Y.D., J.T., B.Y., and Q.G. wrote the original draft. All co-authors performed the review and editing of the final version of the manuscript.

DECLARATION OF INTERESTS

The authors declare no competing interests.

Received: September 27, 2023
Revised: February 8, 2024
Accepted: April 22, 2024
Published: April 24, 2024

REFERENCES

1. McNab, F., Mayer-Barber, K., Sher, A., Wack, A., and O'Garra, A. (2015). Type I interferons in infectious disease. Nat. Rev. Immunol. *15*, 87–103. https://doi.org/10.1038/nri3787.
2. Boxx, G.M., and Cheng, G. (2016). The Roles of Type I Interferon in Bacterial Infection. Cell Host Microbe *19*, 760–769. https://doi.org/10.1016/j.chom.2016.05.016.
3. Mayer-Barber, K.D., and Yan, B. (2017). Clash of the Cytokine Titans: counter-regulation of interleukin-1 and type I interferon-mediated inflammatory responses. Cell. Mol. Immunol. *14*, 22–35. https://doi.org/10.1038/cmi.2016.25.
4. Teles, R.M.B., Graeber, T.G., Krutzik, S.R., Montoya, D., Schenk, M., Lee, D.J., Komisopoulou, E., Kelly-Scumpia, K., Chun, R., Iyer, S.S., et al. (2013). Type I interferon suppresses type II interferon-triggered human anti-mycobacterial responses. Science *339*, 1448–1453. https://doi.org/10.1126/science.1233665.
5. Berry, M.P.R., Graham, C.M., McNab, F.W., Xu, Z., Bloch, S.A.A., Oni, T., Wilkinson, K.A., Banchereau, R., Skinner, J., Wilkinson, R.J., et al. (2010). An interferon-inducible neutrophil-driven blood transcriptional signature in human tuberculosis. Nature *466*, 973–977. https://doi.org/10.1038/nature09247.
6. Zhang, G., Deweerd, N.A., Stifter, S.A., Liu, L., Zhou, B., Wang, W., Zhou, Y., Ying, B., Hu, X., Matthews, A.Y., et al. (2018). A proline deletion in IFNAR1 impairs IFN-signaling and underlies increased resistance to tuberculosis in humans. Nat. Commun. *9*, 85–89. https://doi.org/10.1038/s41467-017-02611-z.
7. Bouchonnet, F., Boechat, N., Bonay, M., and Hance, A.J. (2002). Alpha/beta interferon impairs the ability of human macrophages to control growth of Mycobacterium bovis BCG. Infect. Immun. *70*, 3020–3025. https://doi.org/10.1128/IAI.70.6.3020-3025.2002.
8. Sun, Y., Zhang, W., Dong, C., and Xiong, S. (2020). Mycobacterium tuberculosis MmsA (Rv0753c) Interacts with STING and Blunts the Type I Interferon Response. mBio *11*, e032544-19.
9. Zhang, L., Jiang, X., Pfau, D., Ling, Y., and Nathan, C.F. (2020). Type I interferon signaling mediates Mycobacterium tuberculosis – induced macrophage death. J. Electron Microsc. *218*, e20200887. https://doi.org/10.1084/jem.20200887.
10. Manca, C., Tsenova, L., Freeman, S., Barczak, A.K., Tovey, M., Murray, P.J., Barry, C., and Kaplan, G. (2005). Hypervirulent M. tuberculosis W/Beijing strains upregulate type I IFNs and increase expression of negative regulators of the Jak-Stat pathway. J. Interferon Cytokine Res. *25*, 694–701. https://doi.org/10.1089/jir.2005.25.694.
11. Dorhoi, A., Yeremeev, V., Nouailles, G., Weiner, J., 3rd, Jörg, S., Heinemann, E., Oberbeck-Müller, D., Knaul, J.K., Vogelzang, A., Reece, S.T., et al. (2014). Type I IFN signaling triggers immunopathology in tuberculosis-susceptible mice by modulating lung phagocyte dynamics. Eur. J. Immunol. *44*, 2380–2393. https://doi.org/10.1002/eji.201344219.
12. Wang, J., Hussain, T., Zhang, K., Liao, Y., Yao, J., Song, Y., Sabir, N., Cheng, G., Dong, H., Li, M., et al. (2019). Inhibition of type i interferon signaling abrogates early Mycobacterium bovis infection. BMC Infect. Dis. *19*, 1031. https://doi.org/10.1186/s12879-019-4654-3.
13. Antonelli, L.R.V., Gigliotti Rothfuchs, A., Gonçalves, R., Roffê, E., Cheever, A.W., Bafica, A., Salazar, A.M., Feng, C.G., and Sher, A. (2010). Intranasal Poly-IC treatment exacerbates tuberculosis in mice through the pulmonary recruitment of a pathogen-permissive monocyte/macrophage population. J. Clin. Invest. *120*, 1674–1682. https://doi.org/10.1172/JCI40817.
14. Mayer-Barber, K.D., Andrade, B.B., Oland, S.D., Amaral, E.P., Barber, D.L., Gonzales, J., Derrick, S.C., Shi, R., Kumar, N.P., Wei, W., et al. (2014). Host-directed therapy of tuberculosis based on interleukin-1 and type I interferon crosstalk. Nature *511*, 99–103. https://doi.org/10.1038/nature13489.
15. Sun, L., Wu, J., Du, F., Chen, X., and Chen, Z.J. (2013). Cyclic GMP-AMP synthase is a cytosolic DNA sensor that activates the type I interferon pathway. Science *339*, 786–791. https://doi.org/10.1126/science.1232458.
16. Collins, A.C., Cai, H., Li, T., Franco, L.H., Li, X.D., Nair, V.R., Scharn, C.R., Stamm, C.E., Levine, B., Chen, Z.J., and Shiloh, M.U. (2015). Cyclic GMP-AMP Synthase Is an Innate Immune DNA Sensor for Mycobacterium tuberculosis. Cell Host Microbe *17*, 820–828. https://doi.org/10.1016/j.chom.2015.05.005.
17. Watson, R.O., Bell, S.L., MacDuff, D.A., Kimmey, J.M., Diner, E.J., Olivas, J., Vance, R.E., Stallings, C.L., Virgin, H.W., and Cox, J.S. (2015). The Cytosolic Sensor cGAS Detects Mycobacterium tuberculosis DNA to Induce Type I Interferons and Activate Autophagy. Cell Host Microbe *17*, 811–819. https://doi.org/10.1016/j.chom.2015.05.004.
18. Lienard, J., Nobs, E., Lovins, V., Movert, E., Valfridsson, C., and Carlsson, F. (2020). The Mycobacterium marinum ESX-1 system mediates phagosomal permeabilization and type I interferon production via separable mechanisms. Proc. Natl. Acad. Sci. USA *117*, 1160–1166. https://doi.org/10.1073/pnas.1911646117.
19. Honda, K., Yanai, H., Takaoka, A., and Taniguchi, T. (2005). Regulation of the type I IFN induction: A current view. Int. Immunol. *17*, 1367–1378. https://doi.org/10.1093/intimm/dxh318.
20. Wu, J., and Chen, Z.J. (2014). Innate Immune Sensing and Signaling of Cytosolic Nucleic Acids. Annu. Rev. Immunol. *32*, 461–488. https://doi.org/10.1146/annurev-immunol-032713-120156.
21. Dey, B., Dey, R.J., Cheung, L.S., Pokkali, S., Guo, H., Lee, J.-H., and Bishai, W.R. (2015). A bacterial cyclic dinucleotide activates the cytosolic surveillance pathway and mediates innate resistance to tuberculosis. Nat. Med. *21*, 401–406. https://doi.org/10.1038/nm.3813.
22. Stanley, S.A., Johndrow, J.E., Manzanillo, P., and Cox, J.S. (2007). The Type I IFN Response to Infection with Mycobacterium tuberculosis Requires ESX-1-Mediated Secretion and Contributes to Pathogenesis1. J. Immunol. *178*, 3143–3152. https://doi.org/10.4049/jimmunol.178.5.3143.
23. Cheng, Y., and Schorey, J.S. (2018). Mycobacterium tuberculosis-induced IFN-β production requires cytosolic DNA and RNA sensing pathways. J. Exp. Med. *215*, 2919–2935. https://doi.org/10.1084/jem.20180508.
24. Wiens, K.E., and Ernst, J.D. (2016). The Mechanism for Type I Interferon Induction by Mycobacterium tuberculosis is Bacterial Strain-Dependent. PLoS Pathog. *12*, e1005809–e1005820. https://doi.org/10.1371/journal.ppat.1005809.
25. Weindel, C.G., Bell, S.L., Vail, K.J., West, K.O., Patrick, K.L., and Watson, R.O. (2020). LRRK2 maintains mitochondrial homeostasis and regulates innate immune responses to Mycobacterium tuberculosis. Elife *9*, e51071. https://doi.org/10.7554/eLife.51071.
26. Wang, Q., Zhu, L., Jones, V., Wang, C., Hua, Y., Shi, X., Feng, X., Jackson, M., Niu, C., and Gao, Q. (2015). CpsA, a LytR-CpsA-Psr family protein in Mycobacterium marinum, is required for cell wall integrity and virulence. Infect. Immun. *83*, 2844–2854. https://doi.org/10.1128/IAI.03081-14.
27. Grzegorzewicz, A.E., de Sousa-d'Auria, C., McNeil, M.R., Huc-Claustre, E., Jones, V., Petit, C., Angala, S.K., Zemanová, J., Wang, Q., Belardinelli, J.M., et al. (2016). Assembling of the Mycobacterium tuberculosis Cell Wall Core. J. Biol. Chem. *291*, 18867–18879. https://doi.org/10.1074/jbc.M116.739227.
28. Malm, S., Maaß, S., Schaible, U.E., Ehlers, S., and Niemann, S. (2018). In vivo virulence of Mycobacterium tuberculosis depends on a single homologue of the LytR-CpsA-Psr proteins. Sci. Rep. *8*, 3936. https://doi.org/10.1038/s41598-018-22012-6.
29. Köster, S., Upadhyay, S., Chandra, P., Papavinasasundaram, K., Yang, G., Hassan, A., Grigsby, S.J., Mittal, E., Park, H.S., Jones, V., et al. (2017). Mycobacterium tuberculosis is protected from NADPH oxidase and LC3-associated phagocytosis by the LCP protein CpsA. Proc. Natl. Acad. Sci. USA *114*, E8711–E8720. https://doi.org/10.1073/pnas.1707792114.
30. Nicholls, S.E., Winter, S., Mottram, R., Miyan, J.A., and Whetton, A.D. (1999). Flt3 ligand can promote survival and macrophage development without proliferation in myeloid progenitor cells. Exp. Hematol. *27*, 663–672. https://doi.org/10.1016/S0301-472X(98)00072-1.
31. Dupont, C.D., Harms Pritchard, G., Hidano, S., Christian, D.A., Wagage, S., Muallem, G., Tait Wojno, E.D., and Hunter, C.A. (2015). Flt3 Ligand Is Essential for Survival and Protective Immune Responses during Toxoplasmosis. J. Immunol. *195*, 4369–4377. https://doi.org/10.4049/jimmunol.1500690.
32. Kinoshita, K., Suzuki, T., Koike, M., Nishida, C., Koike, A., Nunome, M., Uemura, T., Ichiyanagi, K., and Matsuda, Y. (2020). Combined deletions of IHH and NHEJ1 cause chondrodystrophy and embryonic lethality in the Creeper chicken. Commun. Biol. *3*, 144. https://doi.org/10.1038/s42003-020-0870-z.
33. Usha Kalyani, R., Perinbam, K., Jeyanthi, P., Al-Dhabi, N.A., Valan Arasu, M., Esmail, G.A., Kim, Y.O., Kim, H., and Kim, H.-J. (2020). Fer1L5, a Dysferlin Homologue Present in Vesicles and Involved in C2C12 Myoblast Fusion and Membrane Repair. Biology *9*, 386. https://doi.org/10.3390/biology9110386.
34. Novikov, A., Cardone, M., Thompson, R., Shenderov, K., Kirschman, K.D., Mayer-Barber, K.D., Myers, T.G., Rabin, R.L., Trinchieri, G., Sher, A., and Feng, C.G. (2011). Mycobacterium tuberculosis triggers host type I IFN signaling to regulate IL-1β production in human macrophages. J. Immunol. *187*, 2540–2547. https://doi.org/10.4049/jimmunol.1100926.
35. Negishi, H., Taniguchi, T., and Yanai, H. (2018). The interferon (IFN) class of cytokines and the IFN regulatory factor (IRF)

transcription factor family. Cold Spring Harbor Perspect. Biol. *10*, a0284233. https://doi.org/10.1101/cshperspect.a028423.

36. Ding, Y., Bei, C., Xue, Q., Niu, L., Tong, J., Chen, Y., Takiff, Howard E., Qian, G., and Bo, Y. (2023). Transcriptomic Analysis of Mycobacterial Infected Macrophages. Infect. Immun. *91*, e0015523. https://doi.org/10.1128/iai.00155-23.
37. Chai, Q., Wang, X., Qiang, L., Zhang, Y., Ge, P., Lu, Z., Zhong, Y., Li, B., Wang, J., Zhang, L., et al. (2019). A Mycobacterium tuberculosis surface protein recruits ubiquitin to trigger host xenophagy. Nat. Commun. *10*, 1973. https://doi.org/10.1038/s41467-019-09955-8.
38. Lerner, T.R., Queval, C.J., Fearns, A., Repnik, U., Griffiths, G., and Gutierrez, M.G. (2018). Phthiocerol dimycocerosates promote access to the cytosol and intracellular burden of Mycobacterium tuberculosis in lymphatic endothelial cells. BMC Biol. *16*, 1. https://doi.org/10.1186/s12915-017-0471-6.
39. Paz, I., Sachse, M., Dupont, N., Mounier, J., Cederfur, C., Enninga, J., Leffler, H., Poirier, F., Prevost, M.C., Lafont, F., and Sansonetti, P. (2010). Galectin-3, a marker for vacuole lysis by invasive pathogens. Cell Microbiol. *12*, 530–544. https://doi.org/10.1111/j.1462-5822.2009.01415.x.
40. Wassermann, R., Gulen, M.F., Sala, C., Perin, S.G., Lou, Y., Rybniker, J., Schmid-Burgk, J.L., Schmidt, T., Hornung, V., Cole, S.T., and Ablasser, A. (2015). Mycobacterium tuberculosis Differentially Activates cGAS-and Inflammasome-Dependent Intracellular Immune Responses through ESX-1. Cell Host Microbe *17*, 799–810. https://doi.org/10.1016/j.chom.2015.05.003.
41. Watkins, B.Y., Joshi, S.A., Ball, D.A., Leggett, H., Park, S., Kim, J., Austin, C.D., Paler-Martinez, A., Xu, M., Downing, K.H., and Brown, E.J. (2012). Mycobacterium marinum SecA2 promotes stable granulomas and induces tumor necrosis factor alpha in Vivo. Infect. Immun. *80*, 3512–3520. https://doi.org/10.1128/IAI.00686-12.
42. Gan, Z., Chen, S.N., Huang, B., Zou, J., and Nie, P. (2020). Fish type I and type II interferons: composition, receptor usage, production and function. Rev. Aquacult. *12*, 773–804. https://doi.org/10.1111/raq.12349.
43. Hoffpauir, C.T., Bell, S.L., West, K.O., Jing, T., Wagner, A.R., Torres-Odio, S., Cox, J.S., West, A.P., Li, P., Patrick, K.L., and Watson, R.O. (2020). TRIM14 Is a Key Regulator of the Type I IFN Response during Mycobacterium tuberculosis Infection. J. Immunol. *205*, 153–167. https://doi.org/10.4049/jimmunol.1901511.
44. Ni, G., Ma, Z., Wong, J.P., Zhang, Z., Cousins, E., Major, M.B., and Damania, B. (2020). PPP6C Negatively Regulates STING-Dependent Innate Immune Responses. mBio *11*, e017288-20. https://doi.org/10.1128/mBio.01728-20.
45. Ni, G., Konno, H., and Barber, G.N. (2017). Ubiquitination of STING at lysine 224 controls IRF3 activation. Sci. Immunol. *2*, eaah7119. https://doi.org/10.1126/sciimmunol.aah7119.
46. Pozos, T.C., and Ramakrishnan, L. (2004). New models for the study of Mycobacterium-host interactions. Curr. Opin. Immunol. *16*, 499–505. https://doi.org/10.1016/j.coi.2004.05.011.
47. Carlsson, F., Kim, J., Dumitru, C., Barck, K.H., Carano, R.A.D., Sun, M., Diehl, L., and Brown, E.J. (2010). Host-detrimental role of Esx-1-mediated inflammasome activation in mycobacterial infection. PLoS Pathog. *6*, e1000895. https://doi.org/10.1371/journal.ppat.1000895.
48. Li, H., Handsaker, B., Wysoker, A., Fennell, T., Ruan, J., Homer, N., Marth, G., Abecasis, G., and Durbin, R.; 1000 Genome Project Data Processing Subgroup (2009). The Sequence Alignment/Map format and SAMtools. Bioinformatics *25*, 2078–2079. https://doi.org/10.1093/bioinformatics/btp352.
49. Anders, S., Pyl, P.T., and Huber, W. (2015). HTSeq-A Python framework to work with high-throughput sequencing data. Bioinformatics *31*, 166–169. https://doi.org/10.1093/bioinformatics/btu638.
50. Movert, E., Lienard, J., Valfridsson, C., Nordström, T., Johansson-Lindbom, B., and Carlsson, F. (2018). Streptococcal M protein promotes IL-10 production by cGAS-independent activation of the STING signaling pathway. PLoS Pathog. *14*, e1006969. https://doi.org/10.1371/journal.ppat.1006969.

STAR★METHODS

KEY RESOURCES TABLE

REAGENT or RESOURCE	SOURCE	IDENTIFIER
Antibodies		
TBK1/NAK Rabbit mAb	ABclonal	Cat#A3458; RRID:AB_2863061
Phospho-TBK1/NAK-S172 Rabbit mAb	ABclonal	Cat#AP1026; RRID:AB_2863910
IRF3 Rabbit pAb	ABclonal	Cat#A2172; RRID:AB_2764190
NF-kB p65/RelA Rabbit mAb	ABclonal	Cat#A19653; RRID:AB_2862717
GAPDH Monoclonal antibody	Proteintech	Cat#60004-1-Ig; RRID:AB_2107436
human Histone-H3 Polyclonal antibody	Proteintech	Cat#17168-1-AP; RRID:AB_2716755
human TIMM44 Polyclonal antibody	Proteintech	Cat#13859-1-AP; RRID:AB_2204679
human Galectin-3 Polyclonal antibody	Proteintech	Cat#14979-1-AP; RRID:AB_2136768
polyclonal Anti-CpsA antibody	Zoonbio Biotechnology	N/A
Anti-GroEL antibody produced in rabbit	Sigma	Cat#G6532; RRID:AB_259939
Bacterial and virus strains		
Wide-type *Mycobacterium marinum* (WT *Mm*)	Obtained from Dr. L. Ramakrishnan. Ramakrishnan L et al.[1]	Cat#ATCC BAA-535
cpsA-deficient *Mycobacterium Marinum* (Δ*cpsA Mm*)	This study	N/A
cpsA-deficient (Δ*cpsA*)_Complementary *Mycobacterium marinum*	This study	N/A
WT *Mm* with green fluorescence	This study	N/A
Δ*cpsA Mm* with green fluorescence	This study	N/A
ΔRD1 *Mm*	Obtained from Dr. L. Ramakrishnan. Ramakrishnan L et al.[1]	N/A
Chemicals, peptides, and recombinant proteins		
Middlebrook 7H9 Broth	BD-Difco	Cat#27131
Middlebrook 7H10 Broth	BD-Difco	Cat#262710
DMSO	Sigma-Aldrich	Cat#D8418
SpeI	NEB	Cat#R3133S
Kanamycin	Sangon Biotech	Cat#A506636
Dulbecco's modified Eagle medium	Gibco	Cat#12491015
NaCl	Sangon Biotech	Cat# A610476
Triton X-100	Sangon Biotech	Cat# A600198
SDS-PAGE Loading Buffer	Cwbio	Cat#CW0027S
EZ-Buffers H 10X TBST Buffer	Sangon Biotech	C520009
BD Difco™ Skim Milk, Bottle, 500g	BD-Difco	Cat#232100
Trizol	Invitrogen	Cat#15596018
Digitonin-water-soluble	Sangon Biotech	A601152
Cell lysis buffer for Western and IP	Beyotime	Cat#P0013
Critical commercial assays		
Nuclear and Cytoplasmic Protein Extraction Kit	Beyotime	Cat#P0027
LDH Cytotoxicity Assay Kit	Beyotime	C0016
GeneJET PCR Purification kit	Thermo Scientific	K0701
Pierce™ BCA Protein Assay Kits	Thermo Scientific	Cat#23225

(*Continued on next page*)

Continued

REAGENT or RESOURCE	SOURCE	IDENTIFIER
TB Green® Premix Ex Taq™ II FAST qPCR	Takara	CN830S
PrimeScript™ RT reagent Kit with gDNA Eraser (Perfect Real Time)	Takara	Cat#RR047A
Experimental models: Cell lines		
RAW 264.7	National Collection of Authenticated cell cultures	CSTR:19375.09.3101MOUSCSP5036
BMDM from WT C57BL/6 mice	Obtained from Dr.Qi Chen(Fujian normal university)	N/A
BMDM from *Cgas* −/− C57BL/6 mice	Obtained from Dr.Qi Chen(Fujian normal university)	N/A
PM from WT C57BL/6 mice	Obtained from Dr.Haipeng Liu (Shanghai Pulmonary Hospital)	N/A
Experimental models: Organisms/strains		
C57BL/6J mice	Sipeifu Biotech	Nifdc
Wild type zebrafish	Obtained from Dr.Bo Yan (Shanghai Public Health Clinial Center, Fudan University)	AB strain
Recombinant DNA		
pPR27-*wasabi*::*cpsA*	This study	N/A
pSMT3:*cpsA*	This study	N/A
Software and algorithms		
GraphPad Prism 9.0	Dotmatics	https://www.graphpad.com
ImageJ	ImageJ	https://imagej.nih.gov/ij/
Samtools	Li et al.[2]	http://samtools.sourceforge.net/
HTseq-count	Anders et al.[3]	https://github.com/simon-anders/htseq
R	R Core Team	https://www.r-project.org/
ggplot2	Posit	https://github.com/tidyverse/ggplot2
Deposited data		
RNA-seq data	This paper	NCBI: PRJNA806763

RESOURCE AVAILABILITY

Lead contact

Further information and requests for resources and reagents should be directed to and will be fulfilled by the lead contact, Dr. Qian Gao (qiangao@fudan.edu.cn).

Materials availability

New plasmids and bacterial strains generated in this study can be obtained by contacting the lead author.

Data and code availability

- The transcriptional profiling data are available at the NCBI: PRJNA806763.
- This study did not generate any original code.
- Data reported in this paper will be shared by the lead contact upon request.

EXPERIMENTAL MODEL AND STUDY PARTICIPANT DETAILS

Animals

A total of 34 six-week-old female C57BL/6J mice were obtained from Sipeifu Biotech (Beijing, China), while 3 six-week-old female *Cgas*$^{-/-}$ C57BL/6J mice were generously provided by Dr. Qi Chen of Fujian Normal University. The mice were housed under standard specific

pathogen-free conditions (24°C, 45%–55% humidity, 12-h light/dark cycle) with free access to water and food. Additionally, 54 adult female zebrafish aged 3–6 months were selected for the study and maintained on a 14-h light/10-h dark schedule. All animal studies followed the ethical review of animal welfare (GB/T 35823-2018). All zebrafish and mouse infection experiments were approved by Laboratory Animal Welfare & Ethics Committee of the Shanghai Public Health Clinical, Fudan University (number 2021-A051-01).

Cell culture

In this study, three types of macrophages were used: the murine macrophage cell line RAW264.7, as well as peritoneal macrophages (PM) and bone marrow-derived macrophages (BMDM). Cells cultured in Dulbecco's Modified Eagle Medium (DMEM; Gibco, USA). All culture media were supplemented with 10% fetal bovine serum (FBS, Gibco, USA) and 1% penicillin-streptomycin solution (FBS, Gibco, USA). The cells were cultured in a 5% CO2 atmosphere at 37°C.

Mycobacterium strains and culture

The *Mm* M strain (ATCC BAA-535) was used as the WT strain.[46] The cultivation and growth measurement of *Mm* strains were performed as described previously.[26]

METHOD DETAILS

The *cpsA* knock out generation and complementation

The *cpsA* knockout strain was generated as previously described with a few modifications.[41] Briefly, 1 kb regions upstream and downstream of the *cpsA* open reading frame (ORF) were PCR amplified genomic DNA of the wild-type *Mm* strain. These two amplified products were ligated to the left and right ends of the kanamycin cassette. The kanamycin cassette used in this study was obtained by PCR amplification from the plasmid pMV306. To obtain the cpsA knockout plasmid, the integrated fragment about 3 kb was amplified using new primers that contained a *Spe*I site. The amplified fragment was then digested with *Spe*I and cloned into the *Spe*I site of the vector pPR27-wasabi. The constructed plasmid was transformed into the wild-type *Mm* strain, and positive clones were selected sequentially using kanamycin and 10% w/v sucrose and fluorescent microscopy. For complementation of Δ*cpsA* strain, the *cpsA* ORF fragment was ligated to the pSMT3 vector. The recombinant plasmid was then transformed into Δ*cpsA Mm* to obtain the complemented strain Δ*cpsA::cpsA Mm*. All of the primers used in this study are listed in Table S1.

Zebrafish infection

Adult zebrafish were infected intraperitoneally with WT *Mm* and Δ*cpsA Mm* as described previously.[26] Briefly, prior to the procedure, the fish were anesthetized using 1x tricaine solution. Using forceps, the fish were gently held by their tails and placed on a sponge-operating table, ensuring that they were securely positioned. A microinjector was then used to inject 10 μL of bacterial suspensions (10^4 colony forming units (CFU)) or PBS into the peritoneal cavity. After injection, the fish were transferred to a new aquarium and maintained at a temperature of 28°C. The fish were fed twice daily and the water was changed every three days. On the eighth day post-infection, the fish exhibited symptoms of ulceration. To euthanize the fish, they were sedated with 25x tricaine for 3 min. Following euthanasia, the fish were fixed in 4% paraformaldehyde for histological analysis and at indicated time points for gene expression analysis.

Mouse tail infection

Nine-week-old female C57BL/6J mice were infected with approximately 3×10^8 CFU of WT *Mm* or Δ*cpsA Mm* in 100 μL PBS via tail vein injection, with an equal volume of PBS used as a control. All mice were sacrificed 10 days post infection, and their tails were collected for subsequent experiments. The tail lesions of eight mice infected with WT *Mm*, Δ*cpsA Mm* or PBS were captured and measured. The total area of tail ulceration in mice tails was calculated using the formula of length × width (cm^2).[47] For analysis of gene expression, the tails were cut into pieces and immediately placed in 1 mL TRIzol reagent in cryogenic vials. Due to the difficulty in digesting mouse tail tissue, 250 μL of 0.1 Mm Zirconia/Silica beads were added to the cryogenic vials, and the mixture was shaken using a Mini Beater shaker at 480 rpm for 30 s. The cryogenic vials were then immediately placed on ice for 5 min. This shaking and cooling process was repeated three times. Afterward, the cryogenic vials were centrifuged at 13,000 g for 10 min, and the supernatant was transferred to a new EP tube. The remaining steps followed the RNA extraction protocol.

Histology

For mice tail infection experiments, the samples were fixed in 4% paraformaldehyde for 48 h, transferred to 75% ethanol. To prepare the samples for further analysis, they were modified to a proper size, which means that the tails were trimmed to a standardized length. This ensures consistency and facilitates subsequent processing steps such as embedding in paraffin. Regarding the zebrafish sample collection, the samples were fixed in 4% paraformaldehyde for 96 h, transferred to 75% ethanol. The heads and tails of the fish were removed to focus on the body portion. The fish body was then divided into 3–4 pieces and embedded in paraffin. The serial sections (5 μm) were prepared and stained with a hematoxylin-eosin (H & E) solution according to the manufacturer's instructions. The histopathology analysis was performed blinded to the experimental group.

RNA extraction and reverse-transcription quantitative PCR (RT-qPCR)

For RNA extraction, 1 mL of TRIzol lysate was transferred to a phase lock gel tube, followed by the addition of 0.4 mL of chloroform. The mixture was vigorously shaken for 10–20 s and then centrifuged at 14,000 g for 15 min at 4°C. The upper layer was carefully transferred to a new RNase-free EP tube, to which 450 μL of isopropanol was added. After inverting the tube to mix, the solution was allowed to precipitate at room temperature for 30 min (or overnight at −80°C). Centrifugation at 14,000 g for 30 min at 4°C resulted in the formation of a visible white precipitate. The supernatant was discarded, and 1 mL of 80% ethanol was added to the precipitate, mixed thoroughly, and centrifuged at 14,000 g for 10 min at 4°C. The supernatant was again discarded, and 1 mL of absolute ethanol was added, followed by shaking and centrifugation at 14,000 g for 10 min at 4°C. After discarding the supernatant, the sample was air-dried on absorbent paper in a well-ventilated area. The RNA was then dissolved in 25–50 μL of water, mixed thoroughly by pipetting, and incubated at 60°C for 5 min to ensure complete dissolution. The concentration of RNA was measured using a Nanodrop, and the RNA was stored at −80°C for long-term preservation. cDNA was synthesized from the RNA using PrimeScript RT reagent Kit with gDNA Eraser kit (TAKARA) according to the manufacturer's instructions, followed by RT-qPCR experiments. RT-qPCRs were carried out in triplicate using TB Green Premix Ex Taq II FAST qPCR (TAKARA) and a CFX96 Real-Time PCR System (Bio-Rad). Target gene expression levels were normalized based on *Gapdh*. Relative RNA levels were calculated by comparative cycle threshold (CT) method ($2^{-\Delta\Delta CT}$ method). ΔΔCT = experimental sample ($CT_{target\ gene}$ - CT_{Gapdh}) - control sample ($CT_{target\ gene}$ - CT_{Gapdh}). The primer sequences of genes measured were listed in Table S2.

Infection of macrophages

Macrophages were infected with *Mm* strains as previously described.[26] The number of host cells used for infection varied depending on the specific experimental objectives. For RNA sample and culture supernatant collection, the infected cells were seeded at a density of 10^6 cells per well (12-well plate). For protein sample collection, the infected cells were seeded at a density of 2×10^6 cells per well (6-well plate). For intracellular bacterial load and immunofluorescence experiments, the infected cells were seeded at a density of 5×10^5 cells per well (24-well plate). Cells were infected with single bacterial suspension at an MOI of 1 for intracellular bacterial load experiments and at an MOI of 10 for other related experiments. Briefly, the infection lasted 4 h, after which the extracellular bacteria were removed with PBS washing twice and further killed with 200 μg/mL gentamicin for 2 h. Subsequently, cells were incubated in fresh medium with 20 μg/mL gentamicin to limit the growth of extracellular bacteria. Samples were collected at indicated time points and subjected to corresponding experiments. All cell infection experiments were conducted at 32°C, as this temperature is optimal for the growth of *Mm*.

RNA sequencing and transcriptome analysis

RNA samples of RAW264.7 cells infected with WT or Δ*cpsA Mm* were collected at 4 hpi and extracted using TRIzol reagent according to the protocol. cDNA libraries were constructed for each sample and sequenced on an Illumina HiSeq 2500 sequencer followed by transcriptome analysis. Sequencing reads were aligned to the mouse reference genome (GRCm38) using HISAT2. Repeated reads in the comparison results were removed using Samtools[48] and expression matrix was obtained through converting to counts using HTseq-count.[49] Principal Component Analysis (PCA) was performed with scatterplot3d package in R. Differentially Expressed Genes (DEGs) in RAW264.7 cells infected with WT or Δ*cpsA Mm* were identified using the limma package (v3.44.3) with a cutoff p value < 0.05, and |fold change| > 2. The data was visualized with Draw Venn Diagram, ggplot2 and Pheatmap in R (v4.0.2). Raw sequencing data were available under accession number NCBI: PRJNA806763.

Western Blot

Whole-cell protein were extracted by solubilizing in Cell lysis buffer for Western and IP (Beyotime) containing PMSF. Nuclear fractions of cells were extracted by Nuclear and Cytoplasmic Protein Extraction Kit (Beyotime) according to its protocol. Proteins were separated with 10% or 12% SDS-PAGE and transferred onto NC membranes after the addition of 5×protein loading buffer, boiled for 10 min. The membranes were blocked by 5% skim milk for 1 h at room temperature (RT). Then, membranes were incubated with specific primary antibodies overnight at 4°C and secondary antibodies for 2 h at RT. Membranes were washed three times with TBST when the end of incubation with antibodies, 10 min each time. The protein signal was detected and analyzed via an Odyssey Infrared scanner (Li-Cor Biosciences, Lincoln, NE). Quantitative analysis was performed with ImageJ software.

Immunofluorescence microscopy (IF)

Cells were seeded at a density of 5×10^5 cells per well (24-well plate) in DMEM (Gibco) supplemented with 10% FBS. After cells were infected with *Mm-Wasabi* for the indicated times, they were fixed with 4% paraformaldehyde (PFA), permeabilized with 0.1% Triton X-100, and then stained with anti-Galectin-3 and Alexa 594-conjugated secondary antibody before confocal microscopy. The cells were imaged with a confocal microscope (Leica SP8).

Lactate dehydrogenase (LDH) release assay

The release of LDH from RAW264.7 cells infected with different *Mm* strains was measured using LDH Cytotoxicity Assay Kit (Beyotime) according to the manufacturer's protocol. Relative cytotoxicity was calculated using the following equation: Cytotoxicity (%) = % of LDH released from the infected cells/maximum LDH released.

Extraction of cytosolic DNA followed by qPCR

Cytosolic DNA and whole cell DNA were extracted from macrophages at 4 hpi as previously described.[50] Briefly, RAW 264.7 cells were washed with PBS once and each sample was divided into two aliquots for whole cell DNA and cytosolic DNA preparation. For whole cell lysates, cells were resuspended in 200 μL 50 μM NaOH (Sangon Biotech), and boiled for 30 min and then neutralized with 20 μL 1M Tris-HCl (pH8). For cytosolic samples, cells were first centrifuged at 500 g for 5 min, and the pellets were resuspended in 500 μL digitonin buffer (25 μg/mL digitonin [Sangon Biotech], 50 mM HEPES [Sangon Biotech], 150 mM NaCl [Sangon Biotech]) for 10 min on ice, followed by centrifugtion at 1000 g for 3 min to collect the supernatant. This step was repeated 3 times and then collect the supernatant by centrifugation at 17000 *g* for 10 min. DNA in the WCL and cytosolic fractions was extracted using the GeneJET PCR Purification kit (Thermo Scientific) and then quatified by qPCR. Host cell mitochondrial and nuclear DNA were quantified by D loop1 and Tert qPCR, respectively. *Mm* genomic DNA was examed by FurA qPCR. The CT values of cytosolic DNA was normalized to the corresponding CT of WCL DNA. For quality control, proteins in the WCL and purified cytosolic fraction were precipitated using 5×protein loading buffer, and analyzed by Western blot using antibodies against GAPDH,TIMM44 (mitochondrial protein) and Histone H3 (nuclear protein) to confirme the cytosolic fractions were free from nuclear and mitochondrial components. The primer sequences of genes measured were listed in Table S2.

QUANTIFICATION AND STATISTICAL ANALYSIS

The unpaired *t* test, Mann-Whitney rank-sum test, One-way ANOVA with Tukey's multiple comparisons test and two-way ANOVA with multiple comparisons were applied to assess the statistical significance using GraphPad Prism 9 software, accordingly.